Assessing Drought Growing-Season in the Kurdistan Region of Iraq Using Integrated Evapotranspiration and Vegetation Indices

Sara H. Zaki[1*] Heman Abdulkhsleq A. Gaznayee[2]

[1,2]Department of Forestry, College of Agriculture Engineering Science, Salahaddin University, Erbil 44003, Kurdistan Region, Iraq; [1]sara.zaki@su.edu.krd, [2] heman.ahmed@su.edu.krd

***Corresponding author:** sara.zaki@su.edu.krd

Abstract

Drought poses a serious threat to agricultural sustainability and water resource management in arid and semi-arid regions such as the Iraqi Kurdistan Region (IKR).This study aims to develop and apply an integrated, multi-indicator framework for early-season drought assessment in IKR, combining meteorological and remote sensing approaches. Reference evapotranspiration (ETo) for April and May from 2003 to 2012 was estimated using the FAO Penman-Monteith method within CROPWAT 8.0, using long-term climatic data from CLIMWAT across key meteorological stations in Duhok, Erbil, and Sulaymania. Simultaneously, satellite-derived spectral vegetation indices including the Vegetation Condition Index (VCI), Temperature Condition Index (TCI), and Vegetation Health Index (VHI) were calculated using NOAA AVHRR imagery to capture spatial and temporal vegetation stress patterns. The proposed framework demonstrates the value of combining ETo and remote sensing indices for early drought detection in rain-fed agricultural systems. This approach supports proactive decision-making in agricultural planning and drought risk management across the Kurdistan Region. Results indicate substantial interannual variability in both ETo and vegetation indices, with 2008 emerging as the most severe drought year, characterized by extremely low VCI (<40) and TCI (<30) values, alongside elevated ETo levels (>200 mm/month) in several locations. Spatial analyses revealed a north-south gradient in drought severity, with southern areas consistently experiencing higher atmospheric water demand. The integrated use of ETo with VCI, TCI, and VHI provided a robust diagnostic tool for identifying critical drought periods, revealing the compounded impacts of thermal and hydrological stress on agricultural systems.The integrated analysis revealed clear spatiotemporal patterns of early-season drought across the region. A strong inverse correlation was observed between ETo and vegetation indices, particularly in drought-prone areas.

Keywords: Drought assessment; Reference evapotranspiration (ETo); Vegetation Indices Remote sensing; and Iraqi Kurdistan Region.

1. Introduction

Drought is a recurring and complex climatic event that significantly impacts agriculture, water resources, and ecological balance, especially in arid and semi-arid areas like the Iraqi Kurdistan Region (IKR) [1]. Agricultural drought, which mainly involves a substantial decrease in soil moisture and evapotranspiration compared to the water needs of crops, can greatly reduce crop yields and overall farming productivity during key growth stages. To accurately and reliably assess agricultural drought, it is essential to combine various climatic and ecological indicators that reflect both weather conditions and plant stress responses.

However, under climate change scenarios characterized by rising temperatures and altered rainfall distribution, these indices often fail to capture the full spectrum of drought impacts. In contrast, reference evapotranspiration (ETo), which reflects atmospheric demand for moisture based on variables like temperature, solar radiation, wind speed, and humidity, offers critical insights into the evaporative stress placed on vegetation and soil. Integrating ETo with satellite-derived vegetation indices provides a more dynamic and responsive approach to monitoring drought conditions in a warming and increasingly variable climate [2]. Including reference evapotranspiration (ETo) in drought assessment methods provides a more detailed understanding of atmospheric water demand, helping to better identify crop-specific water stress. Moreover, using satellite-derived vegetation indices such as the Vegetation Condition Index (VCI), Temperature Condition Index (TCI), and Vegetation Health Index (VHI) improves drought evaluation by offering timely, continuous, and wide-area monitoring of plant health and thermal stress [3], [4].

Although GOES‑19 officially became the operational GOES East satellite on April 7, 2025, satellite data were available before this date in a provisional or pre-operational capacity. Following its launch as GOES‑U on June 25, 2024, and its subsequent transition to GOES‑19 upon reaching geostationary orbit in July 2024, the satellite underwent a series of calibration, testing, and validation procedures. During this period, early data products were made publicly accessible by NOAA and NESDIS, though they were not yet classified as operational. These preliminary datasets, while useful for research and system verification, may differ in quality or completeness compared to post-operational data. Therefore, users accessing GOES‑19 data before April 7, 2025, should be aware of its provisional status.[5].

The integration of reference evapotranspiration (ETo) with satellite-derived spectral vegetation indices offers a synergistic and quantifiable framework for enhancing drought detection accuracy, especially in ecologically diverse and climate-sensitive areas like the Iraqi Kurdistan Region (IKR). Indices such as the Vegetation Condition Index (VCI), Temperature Condition Index (TCI), and Vegetation Health Index (VHI) are particularly sensitive to anomalies in vegetation greenness and thermal stress. When combined with ETo anomalies—which capture deviations in atmospheric water demand this approach allows for early identification of drought onset. For instance, VCI values below 35%, coupled with ETo increases of more than 10% above the long-term mean, can signal emerging drought stress with improved spatial and temporal resolution.The atmospheric demand for moisture reflected through reference evapotranspiration (ETo)captures the combined influence of key climatic variables such as temperature, solar radiation, humidity, and wind speed. When integrated with vegetation-based indicators, this metric bridges the gap between supply-side factors (e.g., precipitation and soil moisture) and demand-side drivers (e.g., evaporative potential). This integration facilitates a more comprehensive and actionable understanding of drought dynamics and their ecological consequences, particularly in regions where vegetation response is highly sensitive to climatic variability. [3], [4].

Building on previous research by Gaznayee et al., which demonstrated the effectiveness of remote sensing techniques and spectral indices in assessing drought severity and vegetation response across the IKR [1], [8], this study adopts a multi-indicator framework that combines ETo and vegetation indices to evaluate early-season drought dynamics. Specifically, ETo is estimated using the FAO Penman-Monteith method, while VCI, TCI, and VHI are derived from NOAA AVHRR data to assess April drought conditions over ten years (2003–2012). This integrated approach enhances drought monitoring capabilities by linking atmospheric moisture demand with satellite-based vegetation health indicators, supporting regional strategies for climate adaptation, agricultural planning, and sustainable resource management.

This study uses an integrated, multi-indicator approach based on ETo and satellite-derived vegetation indices (VCI, TCI, and VHI) to evaluate drought conditions across the IKR during the vital early growing season (April) over ten years (2003–2012). The main goals are to identify drought patterns over time and space, assess regional drought severity, and support sustainable farming and environmental management decisions.

2. Materials and Methods

2.1 Study Area

The study focuses on the Iraqi Kurdistan Region (IKR), comprising the governorates of Duhok, Erbil, and Sulaymaniyah. To enhance the geographic clarity and spatial referencing of the study area, coordinate grids representing latitude and longitude have been overlaid on the map. The study area spans a longitudinal range from 40°E to 48°E and a latitudinal range from 30°N to 38°N, encompassing the entire territory of Iraq. Within this frame, the Kurdistan Region, Specifically the governorates of Duhok, Erbil, and parts of Sulaymaniyah, is highlighted in light blue. This geospatial framing not only facilitates accurate localization of the study area but also supports spatial alignment with satellite-derived datasets and climatic models, thereby improving the precision of drought monitoring analyses. The IKR is characterized by a Mediterranean to semi-arid climate, with distinct cold, wet winters and hot, dry summers. Given that agriculture in this region is predominantly rain-fed, the area is particularly susceptible to drought episodes during the growing season from March to October [6].

2.2.Data Sources for

2.2.1. Estimation of Reference Evapotranspiration (ETo)

To assess the reference evapotranspiration (ETo) during the growing season, multiple methodological approaches were employed, combining station-based climatic data, remote sensing sources, and agro-climatological modeling tools. First, the FAO CROPWAT 8.0 software, in conjunction with the CLIMWAT database, was used to extract long-term monthly climatic data for April from 2003 to 2012 for stations geographically representative of the study area, including Erbil, Duhok, and Sulaymaniyah. This method is widely accepted for estimating ETo under various climatic conditions due to its strong physical basis and data adaptability April provides an early-season snapshot of drought conditions, offering valuable insight into initial moisture availability and vegetative stress at the onset of the growing

In this equation, RnR_nRn is the net radiation at the crop surface (MJ m^{-2} day^{-1}), GGG is the soil heat flux density (MJ m^{-2} day^{-1}), TTT is the mean daily air temperature (°C), u2u_2u2 is the wind speed at 2 m height (m s^{-1}), ese_ses is the saturation vapor pressure (kPa), eae_aea is the actual vapor pressure (kPa), Δ\DeltaΔ is the slope of the saturation vapor pressure curve (kPa $°C^{-1}$), and γ\gammaγ is the psychrometric constant (kPa $°C^{-1}$). This method allows for a high level of accuracy in ETo estimation when

seasonCLIMWAT provides essential parameters such as maximum and minimum temperatures, relative humidity, wind speed, and sunshine hours, which were imported into

CROPWAT to compute ETo using the standard FAO Penman-Monteith equation. The study acknowledges the use of CLIMWAT data and the CROPWAT model as a practical approach for estimating reference evapotranspiration (ETo) in data-scarce environments. However, it recognizes the inherent station-centric bias that may arise due to the limited spatial distribution of meteorological stations across the Kurdistan Region's diverse topography. To address this, stations were selected to represent the main agro-climatic zones of Duhok, Erbil, and Sulaymaniyah, though future work will benefit from incorporating higher-resolution gridded datasets or satellite-derived climate variables to enhance spatial coverage. Regarding missing or incomplete climatic inputs, standard procedures within CROPWAT were followed, which include estimating missing variables using built-in empirical methods or default values recommended by FAO[7].

$$ET_0 = \frac{0.408\Delta(R_n - G) + \gamma\frac{900}{T+273}u_2(e_s - e_a)}{\Delta + \gamma(1 + 0.34u_2)}$$

…………1

$$NDVI = \frac{NIR - Red}{NIR + Red}$$

………....2

2.2.2. Spectral Vegetation Indices:

The National Environmental Satellite, Data, and Information Service (NESDIS), operated by NOAA (National Oceanic and Atmospheric Administration), plays a vital role in monitoring environmental variables, including drought, through satellite remote sensing. One of the key systems utilized in drought assessment is the Advanced Very High Resolution Radiometer (AVHRR), onboard NOAA's polar-orbiting satellites, such as the NOAA-15 to NOAA-20 series and Suomi NPP. These satellites provide daily global observations at moderate spatial resolutions (~1.1 km at nadir for Local Area Coverage and ~4 km for Global Area Coverage). The AVHRR sensor collects data across several spectral bands, including the red (Channel 1: 0.58–0.68 µm), near-infrared (Channel 2: 0.72–1.10 µm), and thermal infrared bands (Channels 4 and 5: 10.3–12.5 µm), which are essential for calculating vegetation and thermal indices.

The drought monitoring methodology begins with the computation of the Normalized Difference Vegetation Index (NDVI). NDVI is derived from the red and near-infrared reflectance values using the formula:

This index provides a measure of vegetation vigor and greenness. Once NDVI is calculated, it is used to compute the **Vegetation Condition Index (VCI)**, which quantifies how current NDVI values compare to their long-term historical extremes on a pixel-by-pixel basis. VCI was calculated based on NDVI data obtained from NOAA AVHRR satellites following the methodology outlined by Kogan [3].:

$$VCI = 100 \times \frac{NDVI - NDVI_{\min}}{NDVI_{\max} - NDVI_{\min}}$$

…..3

where NDVImin and NDVImax represent the historical minimum and maximum NDVI values over a reference period (commonly 1985–2020). VCI values close to 100 indicate very good vegetation health, while values near 0 suggest severe drought conditions.The NESDIS satellite algorithms like VIIRS Surface Reflectance use sophisticated atmospheric correction routines based on physical models (e.g., 6S radiative transfer with aerosol optical thickness, water vapor, ozone, clouds).They rely on atmospheric look-up tables that parameterize aerosol and molecular scattering and absorption, enabling correction of top‑of‑atmosphere reflectance to surface reflectance .Similarly, aerosol detection products (e.g., ABI Aerosol Detection) separate dust and smoke using spectral thresholds, enhancing atmospheric screening,star.nesdis.noaa.gov

Parallel to VCI, the **Temperature Condition Index (TCI)** is derived using thermal infrared brightness temperature (BT) data, which reflect land surface temperature. TCI assesses thermal stress on vegetation by comparing current BT to its historical range, **TCI** was derived from satellite-based brightness temperature measurements using thermal infrared imagery [4]:

$$TCI = 100 \times \frac{BT_{\max} - BT}{BT_{\max} - BT_{\min}} \quad \text{………..…4}$$

Here, a low TCI indicates higher thermal stress and drought severity, while a high TCI represents cooler, less stressful conditions. Both VCI and TCI are essential because vegetation response to drought is influenced not only by moisture stress but also by thermal conditions, especially during the growing season.

The **Vegetation Health Index (VHI)** combines VCI and TCI to produce a more holistic measure of drought impact on vegetation.

These indices were sourced from NOAA's Global Vegetation Health Products (GVHP) with a spatial resolution of 4 km.
GOES-19 Satellite Data: Imagery and data post-2025 from NOAA STAR GOES were utilized to evaluate emerging capabilities for operational drought monitoring [5].

VHI is formulated as:

$$VHI=a\cdot VCI+(1-a)\cdot TCI \quad \text{……..5}$$

where aaa is a weighting factor, typically set at 0.5 to assign equal importance to vegetation greenness and thermal stress. VHI values below 40 generally indicate moderate to severe drought, while values above 60 represent healthy vegetation conditions. This index is widely used for agricultural monitoring, drought early warning, and decision-making in water resource management. Using a static value of a = 0.5 may therefore oversimplify ecosystem responses and reduce the precision of drought detection. To improve accuracy, region- or vegetation-specific calibration of the coefficient based on empirical observations or sensitivity analyses can be adopted. This would allow VHI to reflect actual biophysical responses more reliably, enhancing its utility for agricultural monitoring and water resource decision-making.

Data for these calculations are obtained from NOAA’s long-term AVHRR records, available through NESDIS repositories and products such as the Global Vegetation Health Products (GVHP). These are generated weekly and provide global coverage. Processing tools used for deriving these indices include ENVI, ERDAS Imagine, QGIS, R, and Python, often utilizing libraries like GDAL, NumPy, and matplotlib for geospatial and numerical analysis. The data are typically composited over 7-day periods to reduce cloud contamination and noise.

Regarding accuracy, these indices are generally reliable in capturing large-scale drought trends. However, several factors can influence their precision. Cloud cover, atmospheric aerosols, and terrain variability can affect both NDVI and BT values. Sensor calibration and orbital drift over time may also introduce bias if not corrected. Despite these challenges, numerous studies have validated VCI, TCI, and VHI using ground-based meteorological and crop data. For example, VHI has shown high correlation (R^2>0.7) with the Standardized Precipitation Index (SPI) and other drought indices, particularly in semi-arid and agricultural regions.

In summary, NESDIS/NOAA's use of AVHRR satellite data provides an effective and operational methodology for drought assessment through spectral and thermal indicators. The VCI, TCI, and VHI indices, derived from long-term satellite observations, serve as critical tools for monitoring vegetation health, evaluating agricultural conditions, and supporting climate resilience strategies in drought-prone regions.

2.3 Data Processing and Analysis

Satellite-derived indices were composited for April across the study period (2003–2012), representing early-season drought conditions. ETo maps were spatially interpolated and resampled to match the resolution of vegetation indices using bilinear resampling methods in ArcGIS Pro 3.1 and QGIS 3.34.

To address concerns regarding spatial reliability, a comparison was performed between satellite-derived outputs and available ground station data, particularly for variables such as temperature and reference evapotranspiration (ETo). This ground-truth comparison serves as an initial validation step, confirming general agreement in temporal trends and magnitude.

Zonal statistical analyses were performed using cropland masks sourced from the ESA Climate Change Initiative land cover dataset. Temporal drought anomaly trends were evaluated using Python analytical libraries, including NumPy, Pandas, and Matplotlib, facilitating comprehensive statistical and visual analysis. Comparative map layouts were developed to distinctly illustrate drought patterns and trends over two defined periods: 2003–2007 and 2008–2012, enabling clear visualization of temporal changes.

2.4 Validation and Reference Studies

This research approach was grounded in previous drought assessment methodologies validated in the IKR region by Gaznayee et al. [1], Al-Quraishi et al. [8], and Mahdi et al. [9]. These studies confirmed the effectiveness and reliability of spectral vegetation indices such as VCI and VHI in accurately detecting and quantifying drought impacts. Field-based ground observations and ancillary land cover data were further utilized for method validation and calibration.

3. Results and Discussion

The analysis of monthly reference evapotranspiration (ETo) for April and May during the period 2003 to 2012 across various meteorological stations in the Kurdistan Region in Table 1 reveals substantial spatial and temporal variability. Stations located in lowland areas such as Makhmoor, Khabat, and Erbil consistently recorded the highest ETo values, frequently exceeding 200 mm/month, particularly in warmer years such as 2007 and 2012. In contrast, elevated and mountainous locations like Rawanduz, Soran, and Amadia exhibited comparatively lower ETo values, often below 150 mm/month, likely due to cooler temperatures and greater humidity.

Table 1: Monthly ETo (mm/month) for April and May (2003–2012)

STATION	Longitude	Latitude	2003	2004	2005	2006	2007	2008	2009	2010	2011	2012
Akre	**43.89333**	**36.74139**	135.8	148.7	146.6	133.2	138.0	136.5	148.3	120.5	164.4	175.9
Amadia	**43.48722**	**37.09250**	116.8	111.0	118.8	115.1	108.3	121.0	116.8	110.7	113.2	101.3
Ankawa	**43.99356**	**36.24293**	160.2	156.9	168.9	144.6	159.1	197.6	184.9	176.0	166.8	180.4
Batel	**42.72165**	**36.95946**	151.6	156.8	141.7	125.8	134.0	166.3	138.3	164.2	142.4	141.1
Duhok	**42.97900**	**36.86790**	144.2	136.4	141.7	135.4	115.9	123.1	129.7	122.4	111.4	126.7
Sarsink	**43.35028**	**37.05028**	121.8	110.6	121.4	113.4	106.9	110.6	112.7	109.3	110.4	116.8
Zakho	**42.68191**	**37.14361**	132.2	123.9	129.2	125.9	118.8	129.7	121.7	122.3	125.4	126.0
Zaweta	**43.14278**	**36.90583**	129.3	125.7	130.6	120.6	113.5	115.0	128.4	118.9	117.7	129.0
Bazian	**45.13952**	**35.58902**	107.6	101.2	117.1	116.9	107.3	134.8	112.2	105.5	100.5	129.9
Chamchamal	**44.83333**	**35.53333**	121.3	100.4	99.8	144.5	159.0	110.0	101.7	101.8	97.6	142.0
Chwarta	**45.57472**	**35.71972**	146.5	126.1	157.1	141.6	130.1	179.0	140.5	146.0	137.5	151.3
Darbandikhan	**45.68625**	**35.11626**	160.7	146.2	161.3	147.9	152.7	178.7	156.3	157.6	156.9	182.9
Dukan	**44.95278**	**35.95417**	156.2	141.9	142.9	131.7	139.9	178.6	171.8	159.2	153.5	189.7
erbil	**43.98391**	**36.21885**	167.0	176.3	154.2	145.8	152.1	189.1	165.8	161.7	145.8	200.9
Halabja	**45.97389**	**35.18639**	146.5	133.2	156.1	140.4	125.6	180.6	140.6	139.5	136.6	164.7
Khabat	**43.67389**	**36.27278**	157.4	136.9	144.5	130.6	140.8	167.0	139.0	148.3	150.3	155.6
Kifri	**44.96639**	**34.68333**	201.1	194.0	181.6	177.2	200.9	193.6	179.1	170.9	189.0	167.0
Koya	**44.64806**	**36.09944**	159.9	139.8	146.5	150.6	133.6	164.2	140.4	134.4	143.8	140.7
Makhmoor	**43.58330**	**35.78330**	210.3	215.9	235.7	221.2	228.4	250.7	217.0	216.1	213.3	226.1
Mangish	**43.09252**	**37.03513**	125.3	125.6	126.5	121.1	109.7	130.6	127.1	123.0	121.2	129.7
Penjwen	**45.94139**	**35.61972**	116.5	84.8	131.5	109.6	113.7	112.8	113.8	118.7	125.2	149.1
Rwanduz	**44.52472**	**36.61194**	113.2	125.4	117.3	122.8	126.8	105.6	119.2	130.7	123.6	108.6
salahaddin	**44.21097**	**36.37468**	155.7	132.7	144.8	129.8	118.0	149.4	140.2	129.7	117.3	138.6
Shaqlawa	**44.00917**	**36.19111**	145.0	123.3	133.3	140.9	142.2	168.0	133.3	129.0	133.5	142.1
sharia	**42.96349**	**36.78414**	108.2	120.5	107.5	113.0	129.0	108.2	108.7	121.4	132.5	117.5
Soran	**44.56136**	**36.63846**	137.4	119.6	132.2	123.4	120.4	148.2	131.4	118.2	124.8	143.5
Sulaymaniyah	**45.43556**	**35.55722**	125.9	90.9	129.6	125.7	118.2	143.4	122.1	114.0	112.4	128.3

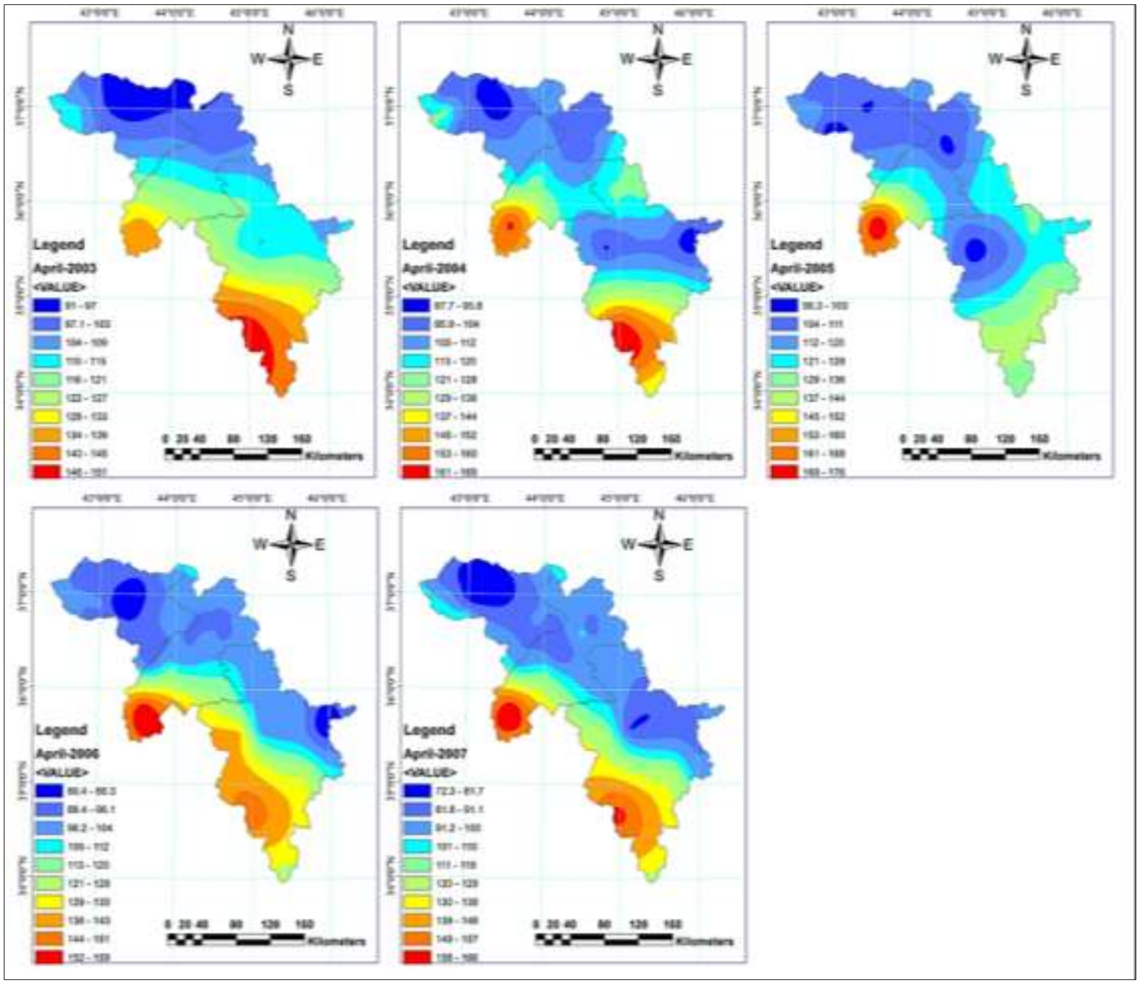

Figure 1: Spatial Distribution of Reference Evapotranspiration (ETo) in the Iraqi Kurdistan Region for April (2003–2007)

The year 2008 stands out as a period of widespread atmospheric dryness, with exceptionally high ETo values across many stations, including Ankawa (197.6 mm), Koya (200.9 mm), and Halabja (180.6 mm), indicating increased evaporative demand. Conversely, years such as 2004 and 2009 showed reduced These findings highlight the influence of local climatic and topographic factors on evapotranspiration and emphasize the importance of ETo monitoring for agricultural planning and water resource management. Regions with persistently high ETo during critical crop development stages face increased irrigation demands and heightened drought risk, necessitating proactive adaptation strategies. ETo values, corresponding to more favorable weather conditions and possibly higher rainfall. Notably, the Makhmoor station exhibited extreme ETo conditions, reaching a peak of 250.7 mm in 2007, underscoring its vulnerability to climatic extremes.

The provided spatial maps illustrate in Figure 1 the temporal and spatial distribution of Reference Evapotranspiration (ETo) across the Iraqi Kurdistan Region (IKR) during April and May for the period from 2003 to 2012. A noticeable variation in ETo values and distribution patterns can be observed over the analyzed years. In April 2003, ETo values ranged from 91 to 151 mm/month, with the highest values concentrated predominantly in the southern and southeastern regions. This spatial pattern indicates higher evaporation rates likely due to warmer temperatures and possibly lower humidity levels in these areas. From 2004 to 2005, an increase in the maximum ETo values is evident, reaching up to 176 mm/month in April 2005.

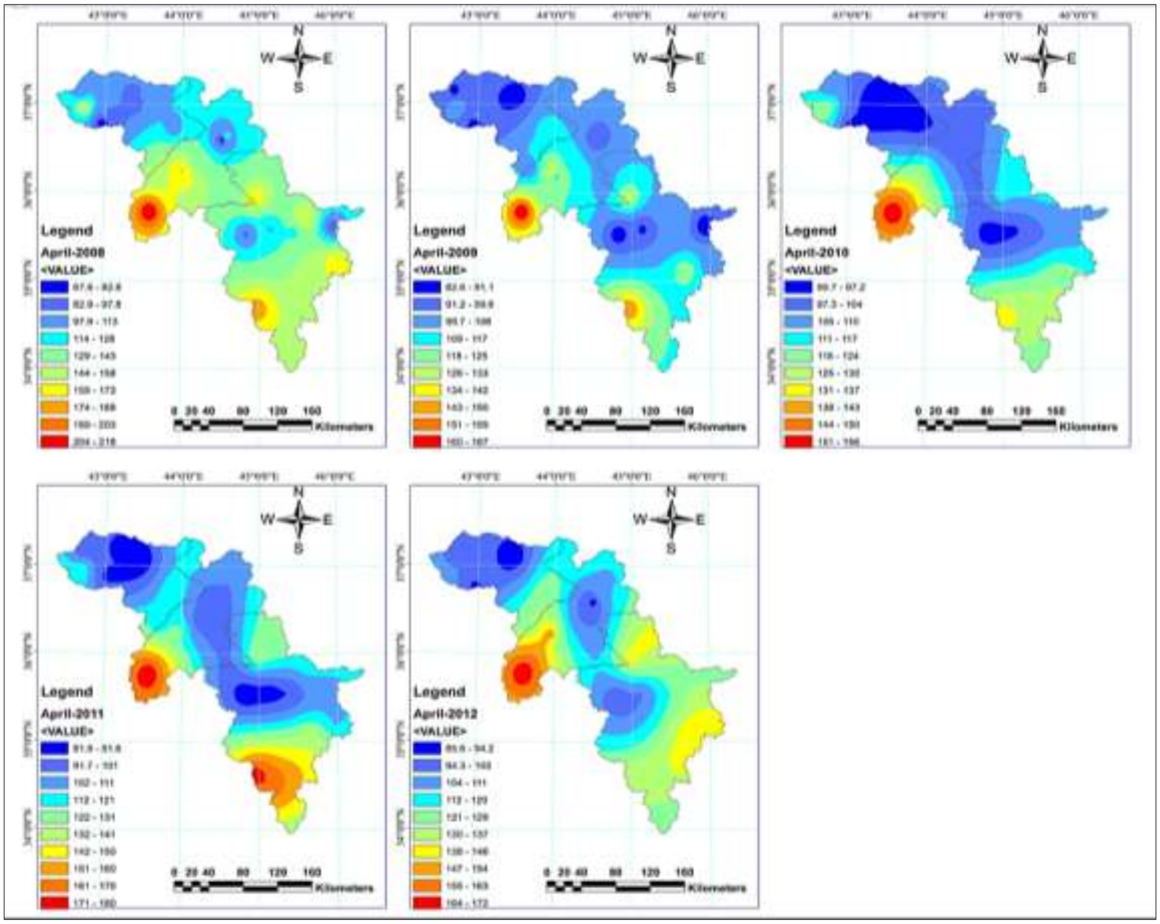

Figure 2: Spatial Distribution of Reference Evapotranspiration (ETo) in the Iraqi Kurdistan Region for April (2008–2012)

High values consistently occur in the southern and southeastern parts, indicating persistent climate conditions that promote higher evapotranspiration rates. The year 2006 shows a slight decrease in the ETo range (80.4 to 159 mm/month), reflecting potential climate variations such as increased humidity or lower temperatures, which tend to suppress evapotranspiration rates. However, in the following years (2007–2012), ETo values generally fluctuated but remained relatively high, surpassing 180 mm/month by April 2008, indicating a return to warmer or drier conditions that boost evapotranspiration. Throughout the study period, the spatial pattern clearly shows a north-to-south gradient, with the highest ETo values mainly found in southern regions. This suggests a climatic gradient, with the southern parts of the IKR experiencing higher evaporation stress, possibly due to differences in elevation, land use, and atmospheric conditions. These practices are essential for maintaining agricultural productivity and environmental stability. The variations over the years highlight significant interannual fluctuations in ETo, likely influenced by broader climatic phenomena. Overall, understanding these temporal and spatial ETo patterns is vital for agricultural management, water resource planning, and drought mitigation. Regions with consistently high ETo may need targeted irrigation and water conservation efforts. Analysis of drought indicators from 2003 to 2012, including the Vegetation Condition Index (VCI), Temperature Condition Index (TCI), and Vegetation Health Index (VHI), shows considerable interannual environmental stress across the provinces of Duhok, Erbil, and Sulaymaniyah. As shown in Figures 3, 4, and 5, these indicators provide a detailed view of the region's fluctuating environmental conditions over this decade-long period. VCI values reveal that moderate vegetation health was dominant, mostly ranging from 50 to 65. This indicates that, for most of the period, vegetation was neither exceptionally healthy nor severely stressed. Notably, in 2008, there was a significant and widespread decline in vegetation health, with the VCI dropping below 40 in all three provinces, signaling a severe drought event. This finding aligns with meteorological data and regional drought reports, as referenced in [10] and [11], underscoring the severity and extent of the drought. After 2008, the VCI showed signs of recovery in 2009 and 2010, exceeding 60, which points to improved vegetation health, likely due to favorable rainfall and positive vegetation response, as discussed in [12]. In contrast to the VCI, the TCI values showed greater variability and generally lower levels throughout the period, indicating that temperature stress was a persistent factor affecting the region's environment. The lower TCI values relative to VCI highlight the ongoing impact of temperature on vegetation health. Specifically, in 2008, TCI sharply decreased to approximately 20–30, reflecting the combined effects of thermal and hydrological drought, detailed in [13]. The simultaneous low VCI and TCI in 2008 emphasize the compounded impact of water scarcity and high temperatures on vegetation health and overall environmental stress.

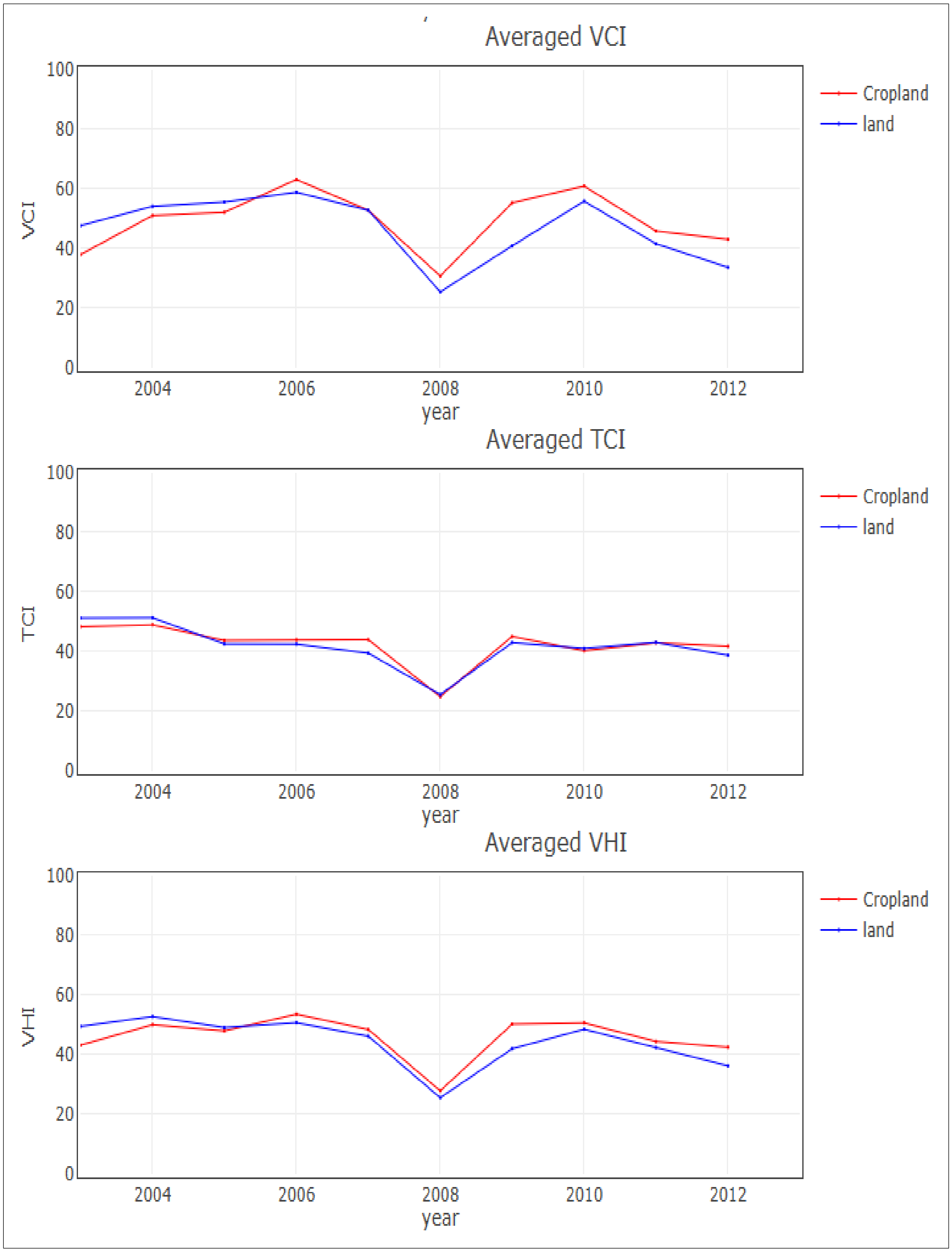

Firure 3: Temporal Variation of Vegetation and Temperature Indices (VCI, TCI, and VHI) for Cropland and Total Land in ERBIL (2003–2012)

Firure 4: Temporal Variation of Vegetation and Temperature Indices (VCI, TCI, and VHI) for Cropland and Total Land in Duhoke (2003–2012)

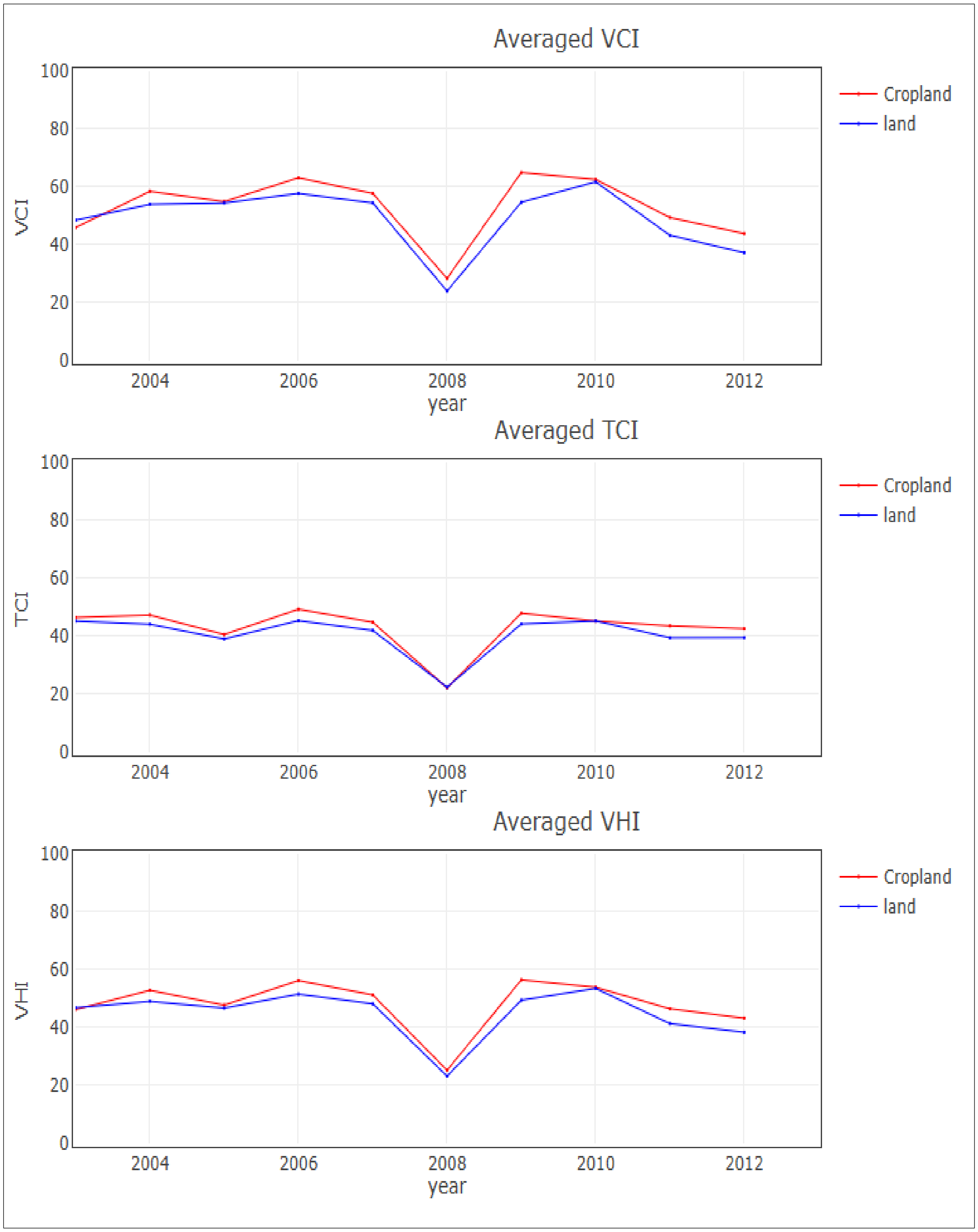

Firure 5: Temporal Variation of Vegetation and Temperature Indices (VCI, TCI, and VHI) for Cropland and Total Land in Sulaymania (2003–2012).

While some recovery occurred in subsequent years, especially during 2009–2010, TCI values remained below optimal, particularly in Sulaymaniya, where prolonged heat stress was observed [14]. These findings are consistent with broader regional and global climate change assessments indicating rising surface temperatures and extended warm periods. The

VHI, which combines VCI and TCI, showed a corresponding stress pattern, with 2008 being particularly critical as VHI fell below 30, marking it as the peak drought year of the decade [16]. The recovery in 2009–2010 and gradual decline in 2011–2012 suggest vegetation's responsiveness to climate improvements and its vulnerability to recurring stress. Cropland areas consistently had slightly higher values across all three indices compared to non-cultivated land, likely due to resilience conferred by irrigation, soil conservation, and adaptive management [17]. Analyzing VCI, TCI, and VHI together effectively captures climatic variability and ecological vulnerability in northern Iraq. The year 2008 stands out as the most severe drought year, emphasizing the importance of monitoring both vegetation and temperature for drought assessment and sustainable land use. To deepen understanding of drought dynamics, this study combines spectral vegetation indices with reference evapotranspiration (ETo), capturing both vegetative and atmospheric drought components. While VCI, TCI, and VHI reflect vegetation response to moisture and thermal stress, adding ETo offers a comprehensive view by considering atmospheric water demand. Calculated via the FAO Penman-Monteith method, ETo indicates potential evapotranspiration under ideal conditions, sensitive to temperature, solar radiation, wind speed, and humidity [18]. Coupling ETo with spectral indices creates a robust framework to evaluate both supply (precipitation and soil moisture) and demand (evaporative loss) aspects of drought. For instance, during the 2008 drought, low VCI values (below 40) combined with high ETo levels reveal a compounded impact of limited rainfall and increased evaporative demand, exacerbating vegetative stress across Duhok, Erbil, and Sulaymaniya. This integrated approach improves drought characterization by linking satellite-derived vegetation responses to the underlying climatic drivers, facilitating early warning and better-informed mitigation strategies [19], [20].

4. Conclusion

This study introduces a comprehensive drought assessment framework that combines reference evapotranspiration (ETo) with satellite-derived spectral vegetation indices (VCI, TCI, and VHI) to evaluate early-season drought conditions across the Iraqi Kurdistan Region (IKR) from 2003 to 2012. The analysis shows the effectiveness of merging atmospheric and vegetation indicators to capture the spatial and temporal variability of drought, especially during the critical early growing season in April. The results highlight 2008 as the most severe drought year, with combined hydrological and thermal stress indicated by very low VCI and TCI values and high ETo levels. Spatial patterns show that the southern parts of the region consistently faced higher evaporative demand, while cropland areas displayed greater resilience, likely due to adaptive management and irrigation practices. This integrated approach effectively characterized both supply-side (precipitation, vegetation moisture) and demand-side (evapotranspiration) drought dynamics, providing a solid framework for regional drought monitoring. Integrating ETo data with vegetation indices improves the understanding of satellite observations by linking vegetation stress to atmospheric water demand. Such a multi-indicator system can serve as a key tool for early warning systems, agricultural planning, and drought mitigation efforts in arid and semi-arid regions.

5. Recommendations

Operationalize Multi-Indicator Monitoring Systems: Environmental and agricultural agencies in the IKR should institutionalize integrated drought monitoring systems using ETo and satellite-based vegetation indices for regular assessments during the growing season.

Early Warning and Risk Management: Develop localized early warning protocols based on threshold values of ETo, VCI, TCI, and VHI to facilitate timely responses and mitigate drought-related impacts on crop productivity. Leverage GOES-19 and Advanced Satellites: Future efforts should incorporate high-resolution data from newer satellites like GOES-19 to enhance the temporal and spatial precision of drought detection and forecasting capabilities. Expand Temporal and Spatial Coverage: Extend the analysis to cover additional months of the growing season (March to October) and integrate more recent datasets (post-2012) to better capture long-term drought trends under evolving climate conditions. Support Adaptive Agriculture: Encourage the adoption of water-efficient practices and climate-resilient crops in regions consistently experiencing high ETo and vegetation stress. Policy Integration: Integrate findings into regional agricultural and water resource policies to support sustainable land management and enhance resilience to climate variability. By adopting these recommendations, policymakers, researchers, and land managers in the IKR can better anticipate, monitor, and respond to drought risks, thereby safeguarding food security and promoting sustainable agricultural development in the region.

Author Contributions: Conceptualization, S.H.; methodology, S.H, resources, S.H, analysis; writing—original draft preparation, S.H; writing—review and editing, S.H.; visualization, and S.H.; supervision, and S.H; funding acquisition, S.H.

Funding: This research was partially funded by Salahaddin University-Erbil

Data Availability Statement: Not applicable.

Acknowledgments: The authors are grateful to all data providers mentioned in the Salahaddin University-Erbil. Lastly, we thank the editors and anonymous reviewers for their insightful comments and recommendations.

Conflicts of Interest: The authors declare no conflict of interest.

References

[1] H. A. A. Gaznayee, A. M. F. Al-Quraishi, and K. Mahdi, "A geospatial approach for analysis of drought impacts on vegetation cover and land surface temperature in the Kurdistan Region of Iraq," *Water*, vol. 14, no. 6, p. 927, 2022. [Online]. Available: https://doi.org/10.3390/w14060927

[2] A. Dai, "Drought under global warming: A review," *WIREs Clim. Change*, vol. 2, no. 1, pp. 45–65, 2011. [Online]. Available: https://doi.org/10.1002/wcc.81

[3] I. Kogan, "Remote sensing of weather impacts on vegetation in non-homogeneous areas," *Int. J. Remote Sens.*, vol. 11, no. 8, pp. 1405–1419, 1990. [Online]. Available: https://doi.org/10.1080/01431169008955102

[4] I. Kogan, "Application of vegetation index and brightness temperature for drought detection," *Adv. Space Res.*, vol. 15, no. 11, pp. 91–100, 1995. [Online]. Available: https://doi.org/10.1016/0273-1177(95)00079-T

[5] NOAA, "GOES-19 now operational as GOES-East," 2025. [Online]. Available: https://www.nesdis.noaa.gov/news/goes-19-operational

[6] Y. K. AL-Timimi, L. E. George, and M. H. AL-Jiboori, "Drought risk assessment in Iraq using remote sensing and GIS techniques," *Iraqi J. Sci.*, vol. 53, no. 4, pp. 1078–1082, 2012. [Online]. Available: https://doi.org/10.24996/ijs.2012.53.4Appendix.%25g

[7] R. G. Allen, L. S. Pereira, D. Raes, and M. Smith, *Crop Evapotranspiration—Guidelines for*

Computing Crop Water Requirements—FAO Irrigation and Drainage Paper 56, Rome, Italy: FAO, 1998.

[8] A. M. F. Al-Quraishi, H. A. A. Gaznayee, and J. P. Messina, "Drought severity trend analysis based on the Landsat time-series dataset of 1998–2017 in the Iraqi Kurdistan Region," in *IOP Conf. Ser.: Earth Environ. Sci.*, vol. 779, no. 1, p. 012083, 2021. [Online]. Available: https://doi.org/10.1088/1755-1315/779/1/012083

[9] M. Riksen, C. J. Ritsema, and K. Mahdi, *Water Management for Climate Smart Agriculture*, 2024. [Online]. Available: https://doi.org/10.3390/books978-3-7258-0619-5

[10] T. Friedrich and A. Kassam, "Low-input intensification of developing countries' agriculture–Opportunities and barriers," *Plant Production and Protection Division, FAO*, Rome, Italy, 2011, p. 115.

[11] Y. K. AL-Timimi, "Drought assessment in Iraq using analysis of Standardized Precipitation Index (SPI)," *Iraqi J. Phys.*, vol. 12, no. 23, pp. 36–43, 2014. [Online]. Available: https://doi.org/10.30723/ijp.v12i23.336

[12] K. A. Abbas, "Drought assessment based on Rainfall Anomaly Index (RAI) across Erbil-Iraq," *Polytech. J.*, vol. 14, no. 1, p. 10, 2024. [Online]. Available: https://doi.org/10.59341/2707-7799.1827

[13] N. Adamo, N. Al-Ansari, V. Sissakian, K. Jehad Fahmi, and S. Ali Abed, "Climate change: Droughts and increasing desertification in the Middle East, with special reference to Iraq," *Engineering*, vol. 14, no. 7, pp. 235–273, 2022. [Online]. Available: https://doi.org/10.59670/ml.v20iS5.4020

[14] H. A. Atiyah, S. M. Khazael, and A. Q. Makhool, "Spatiotemporal drought monitoring using remote sensing technique in Babel-Iraq," *Iraqi J. Sci.*, pp. 1535–1544, 2023. [Online]. Available: https://doi.org/10.24996/ijs.2023.64.3.41

[15] C. B. Field and V. R. Barros, Eds., *Climate Change 2014–Impacts, Adaptation and Vulnerability: Regional Aspects*. Cambridge, U.K.: Cambridge Univ. Press, 2014.

[16] A. A. Damavandi, M. Rahimi, M. R. Yazdani, and A. A. Noroozi, "Assessment of drought severity using vegetation temperature condition index (VTCI) and Terra/MODIS satellite data in rangelands of Markazi Province, Iran," 2016.

[17] M. Goodarzi, J. Abedi-Koupai, M. Heidarpour, and H. R. Safavi, "Development of a new drought index for groundwater and its application in sustainable groundwater extraction," *J. Water Resour. Plann. Manage.*, vol. 142, no. 9, p. 04016032, 2016.

[18] F. N. Kogan, "Application of vegetation index and brightness temperature for drought detection," *Adv. Space Res.*, vol. 15, no. 11, pp. 91–100, 1995.

[19] S. Bachmair, M. Tanguy, J. Hannaford, and K. Stahl, "How well do meteorological indicators represent agricultural and forest drought across Europe?" *Environ. Res. Lett.*, vol. 13, no. 3, p. 034042, 2018.

[20] O. Rojas, A. Vrieling, and F. Rembold, "Assessing drought probability for agricultural areas in Africa with coarse resolution remote sensing imagery," *Remote Sens. Environ.*, vol. 115, no. 2, pp. 343–352, 2011. [Online]. Available: https://doi.org/10.1016/j.rse.2010.09.006